BULLETIN OF THE POLISH ACADEMY OF SCIENCES
TECHNICAL SCIENCES
Vol. 54, No. 4, 2006

Key phenomena in surf and swash zone: process-based modelling and data-driven analysis

J. KAPIŃSKI, R. OSTROWSKI, Z. PRUSZAK*, and G. RÓŻYŃSKI

Institute of Hydro-Engineering, Polish Academy of Sciences, 7 Kościerska St., 80-328 Gdańsk, Poland

Abstract. Selected results of investigations concerning a shallow water part of the coastal zone, covering the surf zone and the swash zone, are presented. The above research has been carried out by means of field measurements, as well as data-driven and theoretical modelling. The investigations have led to development of a mathematical model of wave transformation and run-up on the shore in the Lagrangian system, as well as identification of infragravity waves (edge waves) in the multi-bar morphological beach system and their linkage with rhythmic shoreline forms (cusps). Some empirical relationships have been obtained for the description of number of bars in a bar system and dissipation of wave energy over such morphological structure. The experimental findings are based on field studies carried out at the IBW PAN Coastal Research Station (CRS) in Lubiatowo.

Key words: nearshore zone, waves, sediment motion, coastal morphology and evolution.

1. Introduction

Increasing human pressure on coastal area and more intensive exploration of sea resources in last decades is a reason for a rise of many new concepts and ideas in the domain of process-based modelling and data-driven analysis in the field of coastal engineering. The coastal processes observed and registered *in situ* are crucial for understanding of coastal nature and a basis for validation and verification of theoretical process-based models. Due to continuous technical and technological progress it is now possible to carry out detailed and precise field surveys and obtain analytical solutions of sophisticated systems of equations describing the considered physical processes.

The wind-induced waves, on their way from the deep sea to the seashore vicinity, are subject to a number of transforming processes, such as shoaling, refraction and diffraction, as well as wave energy dissipation. These wave processes, together with the effects of nearshore currents, affect the moveable sandy seabed, which in turn cause evolution of the seabed profile and migration of the shoreline. Within multi-scale morphological forms, dynamically changing in various time-spatial scales, bars play a key role. In a case of the multi-bar shore, there is a system of more or less interacting bars, the activity of which manifests in the processes of wave breaking and energy dissipation, while waves are approaching the seashore. Thus, the bars protect the beach from the erosive impacts of storm waves.

Recently, reasons of coastal evolution have often been assigned not only to the effects of short (wind) waves, but also to longer (infragravity) waves, which can sometimes play a predominant role in nearshore morphodynamics [1]. The infragravity waves typically appear in a very shallow nearshore zone and have periods from tens of seconds to a few minutes. Such waves are generally classified as surf beats which approach the shore almost perpendicularly and edge waves which propagate along the shoreline. The generation and propagation of edge waves are affected by a complicated system of physical phenomena and are extremely difficult in theoretical modelling. The infragravity oscillations are practically hardly visible in direct observations but thorough spectral analyses show that they are a significant component of shallow water wave energy.

While approaching the seashore, the waves gradually lose their energy due to breaking, turbulence and bottom friction. The situation is quite different in case of the long-period oscillations (edge waves), the energy of which increase substantially near the shoreline. The cross-shore distribution of energy of short- and long-period oscillations is shown in Fig. 1.

Recently, the infragravity oscillations, mainly edge waves, have drawn attention of many research teams. There are more and more evidences that these waves play an important role in generation of rip currents, some kind of longshore bars or shoreline rhythmic forms. In 2002 and 2003, a series of field experiments were carried out at the IBW PAN Coastal Research Station (CRS) in Lubiatowo, focused on identification of long-period oscillations of coastal hydrodynamic parameters. The registrations of nearshore waves and currents were accompanied by detailed monitoring of the short-term shoreline evolution.

The coastal zone is a region of occurrence of numerous complex hydro- and morphodynamic processes, because of this, the study is focused only on selected results of investigations of key phenomena, observed in the surf and swash zone, carried out by the authors. A special attention is paid to the verification of hypothesis on the relation between infragravity waves (edge waves) and rhythmic shoreline forms at

*e-mail: zbig@ibwpan.gda.pl

a dissipative multi-bar shore, typical at the south Baltic. Reported in the world literature, the investigations carried out till now were mostly concentrated on shores having a reflective character. The results presented herein are mainly based on the field surveys which were conducted at the Institute of Hydro-Engineering of the Polish Academy of Sciences (IBW PAN) Coastal Research Station (CRS) in Lubiatowo, see Fig. 2.

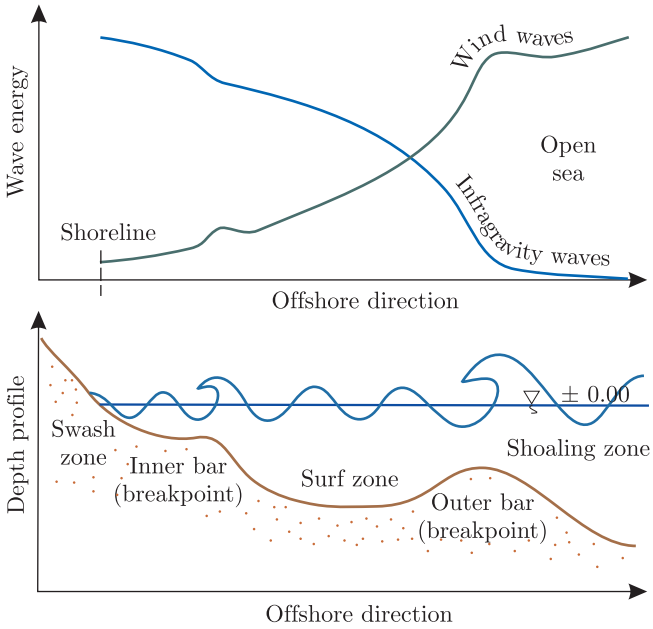

Fig. 1. Cross-shore variability of energy for wind waves and infragravity waves

The records of hydrodynamic parameters at CRS Lubiatowo were taken using automated system, comprising electronic measuring devices, data transmission by cable to a computer, digitisation of signals and storage of digitised data. Water flows were registered by electromagnetic current meters (measurements at points – see dots in Fig. 2), as well as by the Acoustic Doppler Current Profiler (measurements in the water column – see Fig. 2). Waves were identified as instantaneous elevations of water free surface, registered by so-called string wave gauges (see Fig. 2), continuously measuring electric resistance of a vertically submerged part of the 4 m long string.

2. Wave motion

2.1. Wind waves – transformation and dissipation over the bar system. While approaching the shore from the deep sea, waves encounter bars and other large bed forms, which locally decrease water depth rapidly. Consequently, the waves are subject to multiple breaking which in turn causes wave energy dissipation and thus reduction of wave height. At each location of the cross-shore profile, the energy of wave having the length L and height H can be described by the following relationship:

$$E = \frac{1}{8}\rho g H^2 L b \tag{1}$$

The above equation defines wave energy per area of the sea having the length L and the unit width b = 1 m. Comparison of wave energy values registered simultaneously at two chosen locations of the cross-shore transect allows to determine the dissipation of energy of the wave transforming on the distance between these locations. Comparing a local wave energy (E_i) at shallow water with the input (offshore) wave energy (E_o) we can define a certain parameter k_i representing a part of energy which remains after wave transformation from deep water

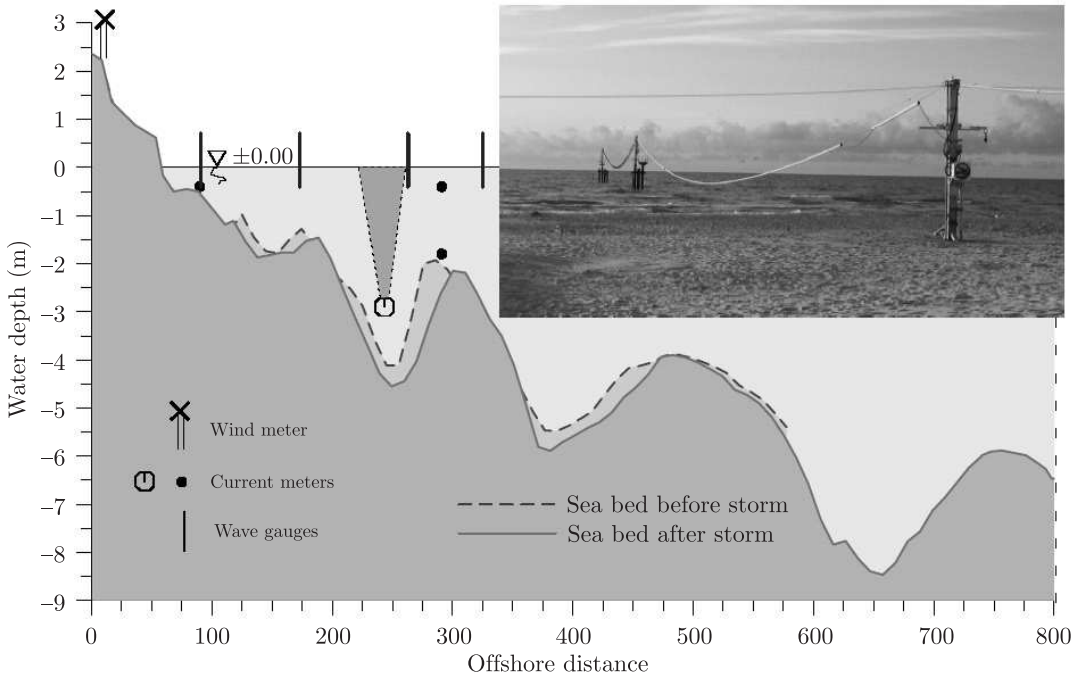

Fig. 2. Sea bed shape and typical locations of measuring devices on the cross-shore profile

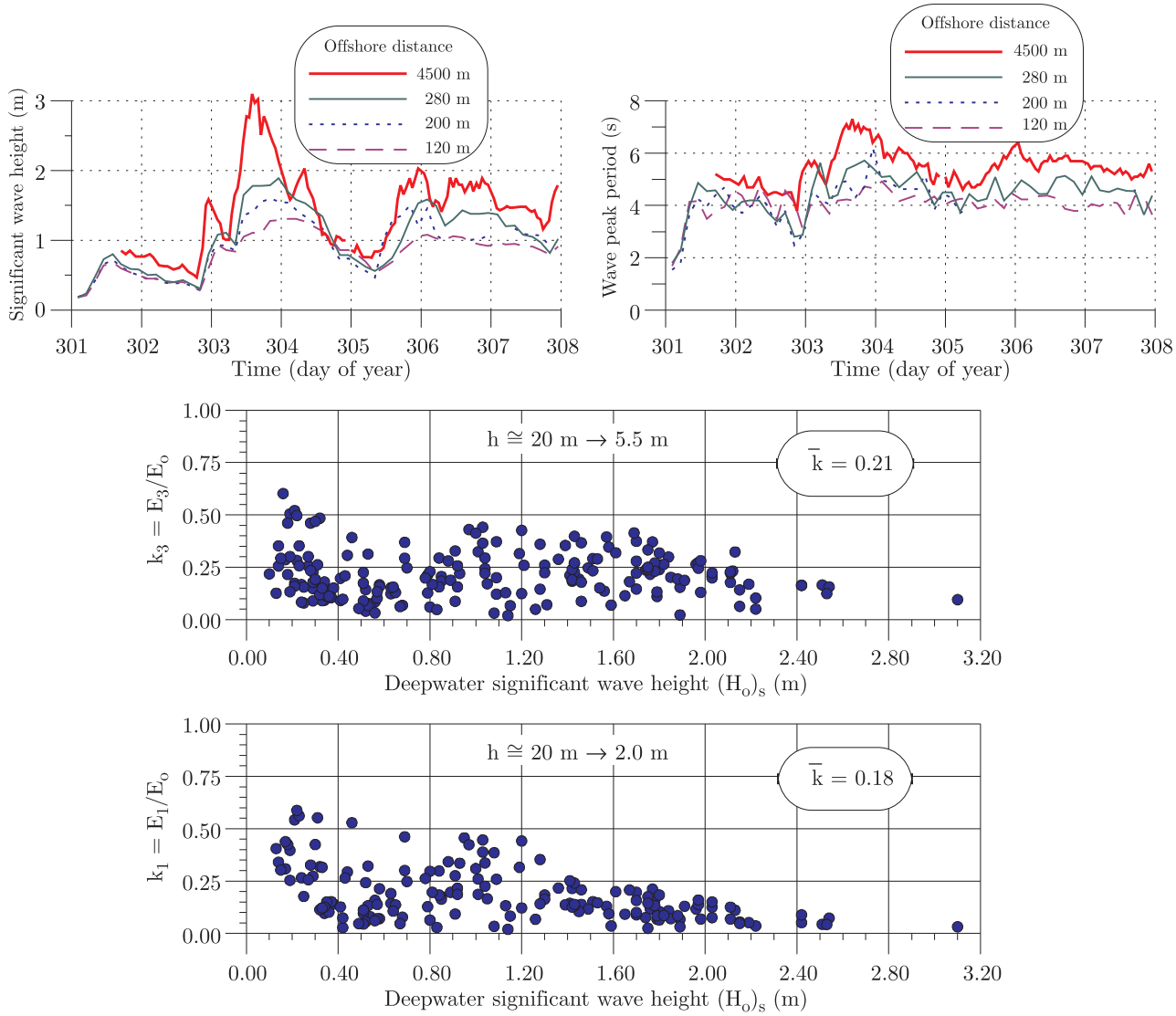

Fig. 3. Exemplary record of changing wave height and period (top) and wave energy dissipation over the multi-bar cross-shore profile as a function of deep water significant wave height (middle and bottom)

depth (h_o) to the nearshore depth (h_i). The field experiments carried out in Lubiatowo show that the coefficient k_i can vary from almost zero to about 0.75, depending on the deepwater significant wave height (see Fig. 3). For higher waves (during a storm) this coefficient is small (great amount of energy dissipates before wave reaches the nearshore zone), while in mild and moderate conditions the offshore bars and shoals do not affect waves and they start to interact with the seabed at relatively shallow water, closer to the shoreline, where rapid wave transformation takes place. Hence, in such conditions, on the way from the offshore regions, a wave height decreases very slowly. For example, an average value of the parameter k_i can amount to $\bar{k}$ = 0.21 for the distance between depths of 20 m and 5.5 m, while for the depth range 20 m – 2 m its value slightly falls to $\bar{k}$ = 0.18 m. When the deepwater significant wave height $(H_0)_s$ exceeds 1.5–2 m, up to 80% of energy is dissipated during wave transformation over three offshore bars (bars II, III and IV). If the deepwater significant wave height exceeds 2.5 m, more than 90% of wave energy reaches the nearshore region. The above quantities denote that during storms not more than 20% of wave energy attains the shoreline vicinity. For smaller input offshore waves, having the significant height $(H_0)_s$ less than 0.5–1.0 m, relatively big amount of energy (from 30% to almost 100%) is passed to the region of bar I and the shoreline proximity.

2.2. Solution of nearshore wave motion in Lagrangian approach. Simulation of a moving shoreline (land-boundary of analysed area) on an inclined beach usually does not constitute any problems for models which are worked out in the Lagrangian method. General equations describing a wave propagation in a two-dimensional horizontal plane can be expressed in the Lagrangian co-ordinates as follows [2]:

$$\frac{\partial^2(h\xi)}{\partial t^2} = -gh\frac{\partial \zeta^L}{\partial x} + \frac{\tau_x^L}{\rho}, \quad \frac{\partial^2(h\psi)}{\partial t^2} = -gh\frac{\partial \zeta^L}{\partial y} + \frac{\tau_y^L}{\rho} \quad (2)$$

$$\frac{\partial^2(\zeta^L)}{\partial t^2} = g\frac{\partial\left(h\frac{\partial\zeta^L}{\partial x}\right)}{\partial x} + g\frac{\partial\left(h\frac{\partial\zeta^L}{\partial y}\right)}{\partial y} - \frac{\frac{\partial\tau_x^L}{\partial x} + \frac{\partial\tau_y^L}{\partial y}}{\rho} \quad (3)$$

where:

x, y – cross-shore and longshore co-ordinates, respectively,

ξ, ψ – cross-shore and longshore components of displacement of a parcel, respectively,

ζ^L – water surface elevation corresponding to an instant position of a parcel,

τ_x^L, τ_y^L – cross-shore and longshore components of a dissipative stress corresponding to an instant position of a parcel, respectively,

h – water depth corresponding to the initial position of a parcel,

ρ, g – water density and acceleration due to gravity, respectively.

In the final equations (model) the wave energy dissipation is expressed by a shear stress at the bottom $\overline{\tau_{fr}^L}$ and by a bore-like breaking at the free water surface $\overline{\tau_{br}^L}$ (the shallow-water and depth-averaged conditions with a hydrostatic distribution of pressure in a vertical direction):

$$\overline{\tau_{fr}^L} = -\frac{1}{2} f\rho \left|\frac{\partial\bar{\rho}}{\partial t}\right| \frac{\partial\bar{\rho}}{\partial t}, \quad (4)$$

$$\overline{\tau_{br}^L} = \begin{cases} 0 & \text{grad}\zeta^L \le S_{br} \\ \rho g h(\text{grad}\zeta^L - S_{br}) & \text{grad}\zeta^L > S_{br} \end{cases} \quad (5)$$

where:

f – friction coefficient,

S_{br} – critical surface steepness of a wave front.

Deepwater waves approaching the shore experience a number of physical phenomena like: refraction, shoaling, diffraction, breaking, bottom friction, run-up and reflection from a beach and finally interference with other incoming waves. All of them have been separately tested to assess the usefulness of the model to forecasting of the shallow-water hydrodynamics. Example of the modelling of the wave refraction is presented in Fig. 4. The regular wave train, characterised by the height H = 1 m and the period T = 10 s, is travelling on the originally undisturbed water surface. The noticeable bending of the wave crests is observed there while running over the underwater mound. So, the subsequent waves adjust their celerity and direction to the contours. Additionally, the effect of the shoaling is observed there in the form of a slight increase of the wave height.

Another example concerns modelling of the diffraction, which appears when a barrier such as a semidetached breakwater interrupts the propagating plane waves. Results of the numerical simulation are presented in Fig. 5. Assuming the same wave train as in the former example, we obtain that the waves which passed by the construction, marked in the figure with a thick solid line, are spreading in the sheltered area. Whereas offshore the plane standing waves are in the course of forming. This phenomena can be explained as the effect of superposition of the incoming waves with the waves, which are reflected from the seaward breakwater's wall.

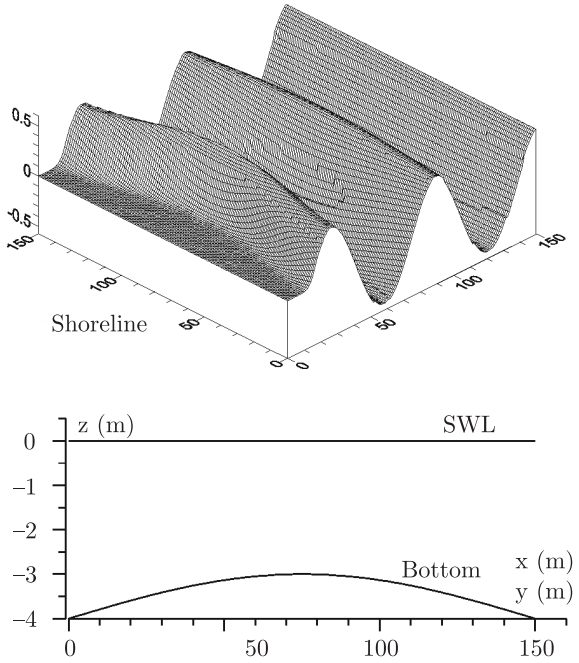

Fig. 4. Wave refraction: bottom contour (up) and bending of wave crests (down)

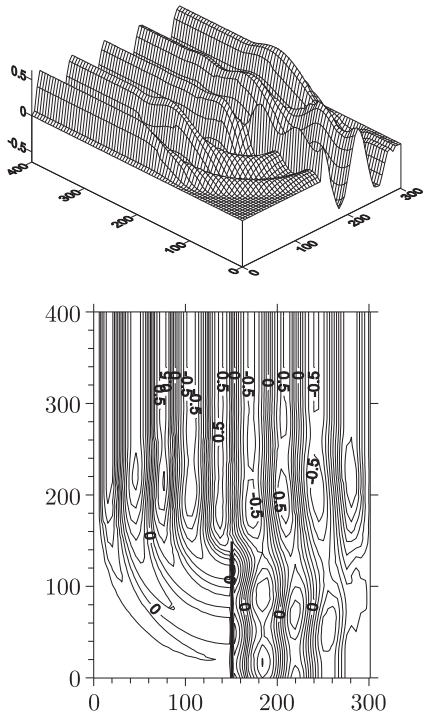

Fig. 5. Wave diffraction: perspective (up) and top view (down)

Waves incoming to the shore usually break evidently altering the pattern of the hydrodynamics. Almost all existing nearshore, time-domain models are worked out for the depth-averaged assumption of motion and the ideal fluid, whereas the wave breaking is clearly the depth-varying and strongly turbulent process. Therefore description of the breaking for this kind of models, despite its complexity, will always be very approximate. In the presented model a geometrical formula of a

bore-like breaking is adopted to avoid steepening of a wave front over an established limitation. Figure 6 shows a several subsequent stages of a breaking wave front, which started 1.4 m from the origin of co-ordinates.

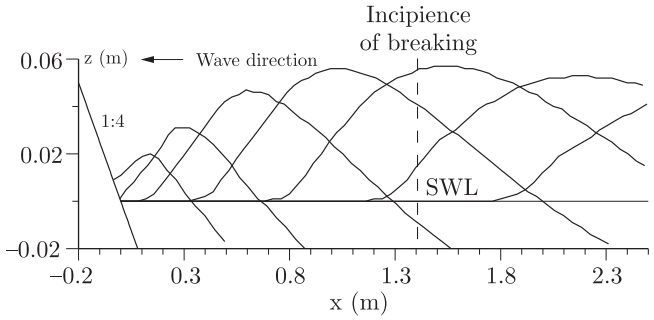

Fig. 6. Modelling of breaking as analogy to bore

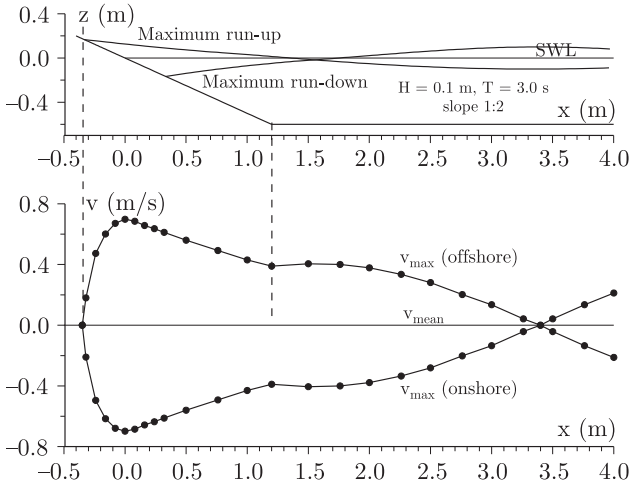

Fig. 7. Water flow velocities for non-breaking wave run-up

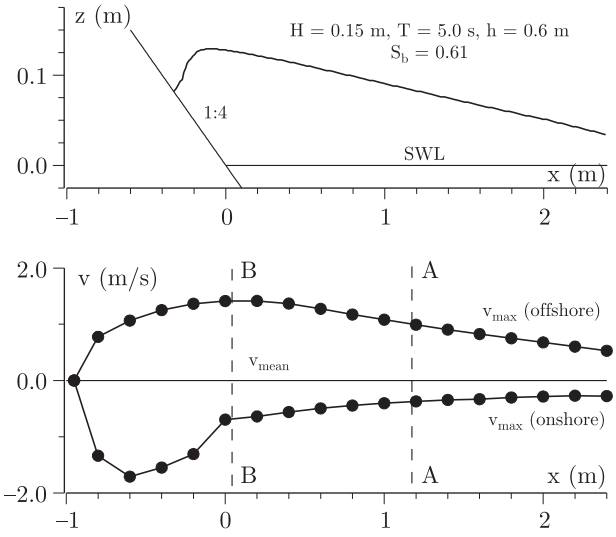

Fig. 8. Water flow velocities for breaking wave run-up

Swash zone is the final region of the wave advance to the shore. Here are observed such wave phenomena like uprush, downrush, reflection and sometimes passing the wave over or through the construction i.e. overtopping and transmission. Moving location of the wave end on a beach slope is usually the trigger for difficulties in extensive time-domain modelling of coastal hydrodynamics. In the presented Lagrangian-type model there is a possibility of an exact mathematical simulation of the water tongue behaviour on a beach slope including the maximum run-up and run-down height.

Possibility of the accurate modelling of the swash zone hydrodynamics allows in-depth analysing such parameters like: displacement and velocity of all parcels, which form the water tongue, as well as step by step transformation of its shape. The conversion of orbital parameters to those, which are representative for constant cross-sections, does not cause difficulty here. Figure 7 presents results of numerical computations of maximum velocity field in the swash zone for non-breaking waves. It is easy to deduce that extreme velocities appear at the junction of *SWL* with the beach slope and that maximum onshore and offshore velocities are symmetrical to one another. Whereas, for the breaking waves running on the beach slope a noticeable asymmetry of the flow velocity pattern is observed. In the example shown in Fig. 8, maximum velocities appear when the run-up phenomenon is in progress.

Modelling of the wave propagation in the Lagrangian method introduces some non-linear effects already in the linear approach. The linear Lagrangian wave advancing in a shallow water is not a pure sinusoid but contains a second order harmonics which results in a flatter trough and steeper crest, however, the wave amplitudes still remain equal to each other. A comparison of the linear and non-linear waves is shown in Fig. 9. The Lagrangian wave shape is more similar to that of the second order Stokes theory especially in the regions of wave crossings.

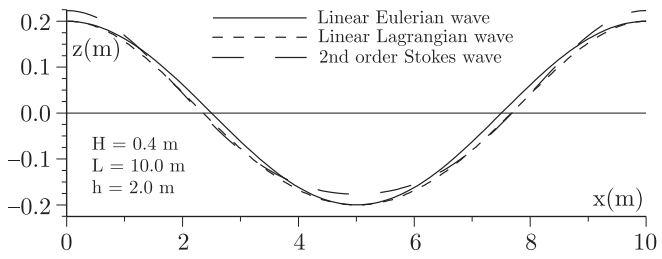

Fig. 9. Comparison of linear Lagrangian and Eulerian waves with 2nd order Stokes theory

2.3. Infragravity waves – statistical and stochastic modelling. The records of water level in close shoreline proximity, described in the Section 1, reflected the wave oscillations in this part of the nearshore region. They were examined statistically to extract long term changes in water table together with slow varying components ω_k of the wave spectrum. The established components can be thought of as characteristic frequencies of infragravity (edge) waves. For their identification results of two field experiments lasting several months each (15^{th} Sept. – 15^{th} Nov. 2002 and 8^{th} Aug. – 15^{th} Nov. 2003) were analysed. They include various hydrological situations ranging

from many days of calm to sequences of heavy storms. Calm periods revealed no slow varying oscillations; in fact they only appeared when deepwater significant wave height exceeded 1 m. In all such cases two clearly visible spectral bands that may account for progressive infragravity waves were identified. Their periods oscillated between $T_k \approx 25$–40 s and $T_k \approx 100$–140 s. Moreover, for more energetic conditions (storm waves), a third less vivid low frequency component emerged corresponding to the period of about Tk=180 s, whereas for higher frequencies another even less clear-cut peak could be identified for $\omega_k = 0.18$ [number of cycles/sampling interval], corresponding to $T_k = 10$–12 s. One of many registrations of deepwater wave height during the analysed stormy period, between 1^{st} and 30^{th} September of 2003, confirms the existence of the mentioned above low-frequency components in shallow water what is presented in Fig. 10.

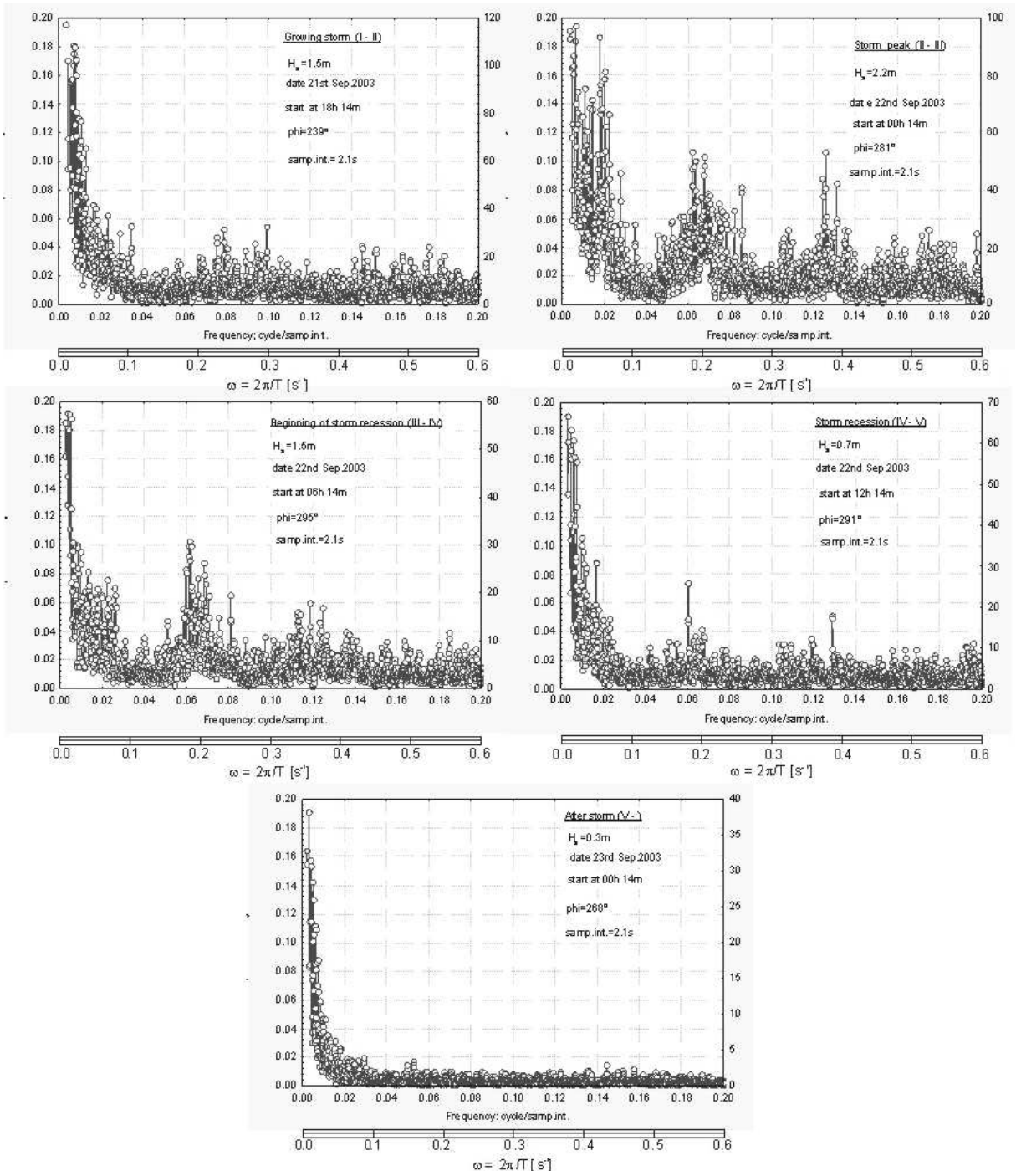

Fig. 10. Exemplary wave spectra with vivid low-frequency peaks

The higher frequencies identified for ω_k = 0.18 are believed to stem from sub-harmonic edge waves, because their periods match the double period of gravity wind waves that predominate at the Lubiatowo beach and that reflect from the shore after having approached it. Interestingly, it was observed that the component with period $T_k \approx$ 25–40 s, depending on changes in wave climate intensity, whereas the component of period $T_k \approx 120$ s, has a more stable structure.

The general equation which links the set of critical (edge) frequencies with local beach characteristic and modal number becomes following shape:

$$\omega_k = \left(\frac{3.5g\beta}{x_o}\right)^{1/2} [(n+1)n]^{1/2}. \tag{6}$$

where n is the modal number, n = 0, 1, 2, ...

The parameter x_o in Eq.(6) denotes a cross-shore length along which the seabed has a constant slope β starting from the shoreline up to a depth h_o. Beyond that distance the depth of seabed is assumed constant and equals h_o. Assuming a Dean type profile described by $x_o = \left(\frac{h_o}{A}\right)^{3/2}$ and a certain characteristic depth $h_o = h_D$, characteristic for a given shore and its dynamics and known as the depth of closure, Eq. (6) can be further transformed to obtain the set of critical (edge) frequencies:

$$\omega_k = \left(\frac{3.5g\beta A^{3/2}}{h_D^{3/2}}\right)^{1/2} [(n+1)n]^{1/2} = C^{1/2}[(n+1)n]^{1/2}. \tag{7}$$

For a local condition defining edge frequencies ((k) it is obtained:

$$\omega_k = 0.0216[(n+1)n]^{1/2}. \tag{8}$$

On the base of the above equation the first modal number, which corresponds to the period of $T \approx 120$ s, is equal $n = 2$, whilst the second one, whose period equals $T \approx 30$ s, is $n = 9$, respectively. That means that for a dissipative multi-bar shore there are only two basic modes connected with infragravity waves. Interestingly, there are no clearly visible waves associated with lower modal numbers ($n = 0$ and 1) which theoretically represent the strongest infragravity components in direct neighbourhood of the shoreline. From the general dispersion relationship:

$$\omega^2 = gK(2n+1)\tan\beta, \quad n = 1, 2, 3, \ldots \tag{9}$$

where K is the wave number and $\omega = 2\pi/T$, the following equation describing the wavelengths of progressive edge waves L_k is obtained:

$$L_k = \frac{g\tan\beta(2n+1)}{2\pi} T_k^2. \tag{10}$$

On the base of this equation we obtained that the wave with $T_k = 120$ s has an alongshore wavelength of some 1700 m, whereas for $T_k = 30$ s the wavelength equals 400 m.

3. Coastal morphodynamics

3.1. Nearshore bars. For the multi-bar coastal zone (with a limited number of 3–5 bars), typical for the south Baltic, we can distinguish two subsystems of bars. The first subsystem comprises inner bars, namely the first two stable bars, while the next bars constitute the outer system of bars. The analysis of behaviour of individual bars within the entire bar system has not provided any distinct correlations between both subsystems of bars. Therefore, it can be assumed that these subsystems behave rather independently. Certain relationships are visible within each subsystem where location and movement of bars are more or less correlated. Such correlations were investigated for distances from shoreline to bar crests or as distances between crests of bar pairs, see Fig. 11. It should be noted that these correlations are bigger when closer to the shore. For instance, the correlation coefficient between bars I and II amounts to $R = 0.57$, while for bars III and IV it is only $R = 0.36$. For the next bars (if there are any more) this correlation decreases rapidly. Similar character of correlations is displayed between behaviour of shoreline and bars belonging to both subsystems. There is a big correlation between bar I and the shoreline ($R = 0.72$), decreasing to $R = 0.30$ for bar II and $R = 0$ for bar IV, Fig. 11. Furthermore, bar I strongly interacts with an additional unstable bar (which can be named "bar 0"). This nearshore bar is very dynamic and disappears frequently. In calm periods, this bar nourishes the beach berm and the emerged part of a beach, practically "crawling out" from the sea, while during storms its sediment is transported seawards and accumulates at the other, more stable bars. In general, it is an ephemeral form, most often occurring 30–40 m from the shoreline, mainly when a storm calms down and some time after it, basically for wave height $H < 1$ m at location of wave breaking. The correlations between inner and outer bars are usually slightly negative (e.g. bar II versus bar III and bar IV), see Fig. 11.

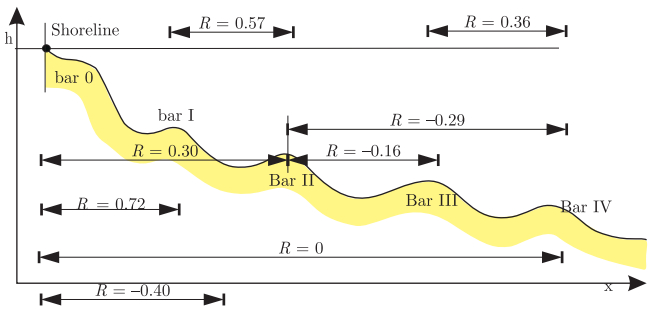

Fig. 11. Correlation between on- and offshore movement of bars

The existence of bars, their magnitude and regularity have a substantial influence on relative stability of shoreline and its erosion rate. Numerous investigations imply that instantaneous lack of a bar due to its destruction during a storm can have catastrophic influence on the seashore when a next severe storm comes before the bar has a chance to rebuilt itself. Such a shore is much more vulnerable to erosion. Longshore continuity and discontinuities of the bars are also very important. Longshore gaps in bar systems are a kind of "energetic windows" through which the deepwater wave energy can be easily transmitted towards the shore. This can lead to local intensive shoreline retreat. Jointly, positions and movements of the

shoreline and the bars constitute a compound dynamic structure of the seashore.

While observing various coastal regions, one can identify both multi-bar shores and the shores totally devoid of bars. Available results of investigations allow one to put forward a hypothesis on existence of two fundamental groups of factors controlling generation of bars and their evolution. The first group comprises environmental passive factors, including mainly sediment features (grain diameter D and density ρ_s), as well as a mean bottom slope in the coastal zone (β), while the second group consists of active parameters, associated with waves and currents, as well as wave transformation and breaking. Assuming that the environmental passive factors are of key importance, as they control the potential possibility of generation of bars and their number on the shore profile, the following general relationship can be postulated:

$$n = f(D, \beta) \approx f(G_\beta). \tag{11}$$

The parameter G_β represents a mass component parallel to the cross-shore slope, associated with the weight of sand grains, described by the following formula:

$$G_\beta = G \tan\beta = (\rho_s - \rho) g D^3 \tan\beta. \tag{12}$$

Taking advantage of available data, the following empirical function approximating Eq. (11) has been obtained (with a correlation coefficient $R = 0.887$):

$$n = 11.42 \left[(\rho_s - \rho) g D^3 \tan\beta\right]^{-0.44} \tag{13}$$

where D is the sediment grain diameter in [m], g – acceleration due to gravity and ρ – water density. A graphical form of Eq. (13) is presented in Fig. 12.

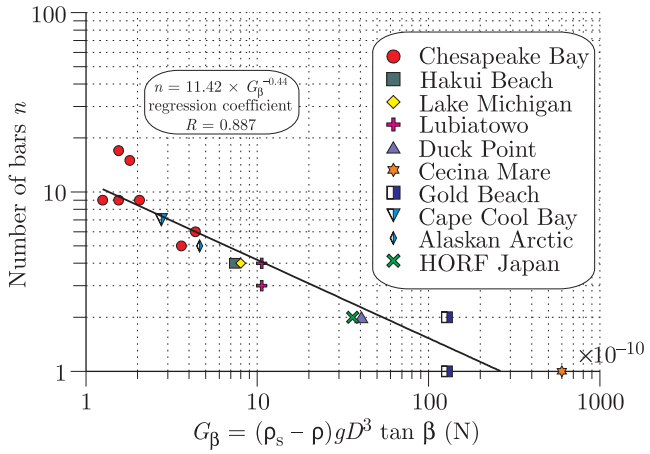

Fig. 12. Number of bars as function of morphological parameters of coastal zone

3.2. Shoreline migration. Long term shoreline migration between 1983 and 1999, see Fig. 13, has been investigated with multi-channel singular spectrum analysis (MSSA), which is a data intensive statistical technique that explores spatial and temporal covariance structure of the studied random field simultaneously. In the studied case the measurements included 27 geodetically referenced shoreline locations equally spanned every 100 m, providing a random field of 27 time series from which the covariance matrix was constructed. This block matrix contained covariances of individual time series along its main diagonal, while cross-covariances among shoreline locations were placed above and beneath the main diagonal, as shown in Eq. (14).

$$\begin{bmatrix} T_{1,1} & T_{1,2} & \dots & T_{1,L} \\ T_{2,1} & T_{2,2} & \dots & T_{2,L} \\ \dots & \dots & \dots & \dots \\ T_{L,1} & T_{L,2} & \dots & T_{L,L} \end{bmatrix} \tag{14}$$

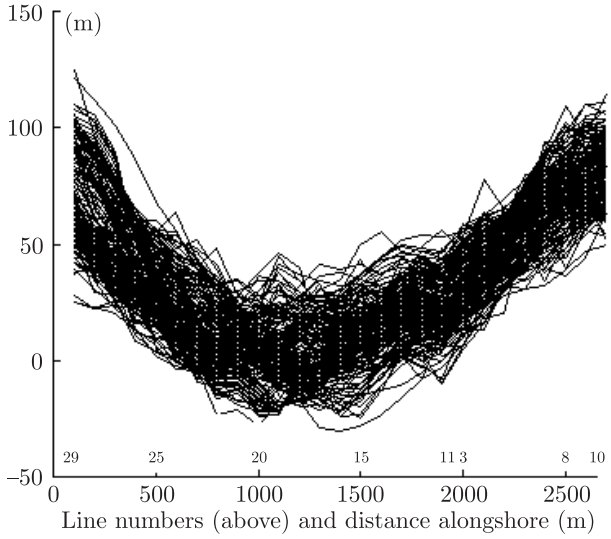

Fig. 13. Envelope of shoreline change at CRS Lubiatowo in 1983–1999

The maximum time lag M is user defined embedding dimension, in combination with L variables forming the analysed random field, the MSSA system matrix is a symmetric $M \cdot L \times M \cdot L$ problem. Analogously to traditional empirical orthogonal functions (EOF), eigenvectors E of the matrix T provide spatial while principal components a yield temporal side of the random field in question. Contrary to the EOF method the MSSA patterns are not unique, which can be established by taking mean values of all ways the system can be reconstructed. For a simple system with $L = 1$ this is shown in Eq. (15a,b,c).

$$(R_\Psi x)_i = \frac{1}{M} \sum_{j=1}^{M} \sum_{k \in \Psi} a_{i-j+1}^k E_j^k \quad \text{for} \quad M \le I \le N - M + 1 \tag{15a}$$

$$(R_\Psi x)_i = \frac{1}{i} \sum_{j=1}^{i} \sum_{k \in \Psi} a_{i-j+1}^k E_j^k \quad \text{for} \quad 1 \le I \le M - 1 \tag{15b}$$

$$(R_\Psi x)_i = \frac{1}{N - i + 1} \sum_{j=i-N+M}^{M} \sum_{k \in \Psi} a_{i-j+1}^k E_j^k \quad \text{for} \quad N - M + 2 \le I \le N. \tag{15c}$$

For Ψ with a single index k, the resulting pattern is called the k-th reconstructed component (RC), which will be denoted

by x^k, the RCs are thus additive, i.e., $R_\Psi x = \sum_{k\in\Psi} x^k$. Hence, the series x can be uniquely expanded as the sum of its RCs:

$$x = \sum_{k=1}^{M} x^k. \tag{16}$$

The RCs are correlated even at lag 0, so variances of RCs are not cumulative.

The MSSA study of shoreline change was done for $L = 27$ shoreline locations evenly spanned along the 2,600 m coastal segment and for the embedding dimension $M = 30$. Western and central locations were enumerated from 29 down to 11, whereas the eastern ones were termed 3 up to 10, which results from the history of local geodetic base at Lubiatowo (the number 3–10 represent the older part while the 29–11 numbers stand for the newer part).

Figure 14 presents the 1st RC of the MSSA analysis for all profiles. For line 29–25 the 1st RC varies in a $\pm$20 m range about the mean empirical shoreline position. For other profiles the 1st RC is not as spectacular but still visible with the range of variations in that portion of the studied coastal segment between +4 and –12 m. The variations have a character of a long standing wave; the lines for profiles 21 and 07 can be regarded as the nodes of that wave, because of their relatively small overall variations. The distance between these two profiles $L = 1.500$ m can be interpreted as the standing wave length. Importantly, there is also a temporal node for all profiles. As it occurred during 16 years (1983–1999), we can say the period of this standing wave is about 32 years. However, this reasoning is entirely based on visual assessment of the 1st RC that embraces only 16 years of observations, so it is safer to judge the period of this standing wave is several decades, see [3].

The 2nd MSSA reconstructed component is demonstrated in Fig. 15. It can be interpreted as standing waves with a period of 7–8 years, with nodes at profiles 27–26 and 16–15. The antinodes can be observed at profiles 22–19 and 03–06. Therefore, a wavelength of 1.000 to 1.300 m can be identified from the locations of nodes and antinodes. The amplitudes are of similar magnitudes ($\pm$10 m), from their extremes the period of 7–8 years could be established. Interestingly, this period coincides with the period of the climatic North Atlantic Oscillation (NAO), so it is possible that its influence is imprinted in shoreline variations of an isolated Baltic Sea.

The inspection of the 3rd MSSA pattern demonstrates a yet another standing wave. From the obtained trajectories we estimate the wavelength to be between 1.400 and 1.600 m and the period between 20–22 years. The magnitude of amplitudes of this standing wave is similar to the amplitudes of the previous two and equals –14 m to +10 m at lines in the centre of the study area, where it is best pronounced, to $\pm$6 m at other lines.

All three patterns represent the forced shoreline response to the wave climate, which consists of standing waves with different wavelengths and periods. Thus, in light of the MSSA study, the wave climate in general can cause the shoreline to perform standing oscillations. Still, the effects of long term wave climate fluctuations can be traced as well (2nd pattern in particular). This is a real progress in the understanding of long term shoreline evolution. Interestingly, locations of nodes and antinodes of these waves appear not to follow any consistent pattern and the evolution at particular spatial points is usually dominated by the most pronounced standing wave at these points, giving the impression that long term shoreline evolution can vary substantially from one sub-segment to another. The MSSA analysis found that in fact the shoreline evolution contains three periodic components at all points.

3.3. Rhythmic shoreline forms (cusps). Field observations of shoreline rhythmic undulations indicate that they incorporate several spatial scales. The smallest ones with wavelengths of several meters, see Fig. 16A, usually occur during calm or mild wave conditions. A system of such forms can occupy shorter or longer pieces of the shoreline. In such instances, the lengths of individual rhythmic forms are in the order of magnitude of the incoming wind waves. Similar rhythmic shoreline forms are also developed in mild swell conditions. Therefore, studies on beach cusps are usually executed to investigate the role of nearshore hydrodynamics in their formation; the current study was focused on that issue.

For the analysed dissipative south Baltic coast and low energy input from waves and currents, the observed cusps usually measured from 6 to 18 m. These quantities are similar to those measured by King on a natural beach with ($\beta = 2.6^\circ$ and swell $T = 9.5$ s, (36 cusps with average spacing of 14.7 m) [4]. Since mechanisms of beach cusp formation are still insufficiently known [4,5] the presence of these forms could be attributed to either sub-harmonic ($T_k = 2T$) and synchronous ($T_k = T$) edge waves or self-organizing processes. It is also possible that both phenomena can co-operate and thus jointly contribute to the appearance of cusps [5].

Assuming that the most common swell in the south Baltic Sea has a period of T_i = 6–9 s and the measured beach slope near the waterline equals tan($\beta \approx$ 0.04–0.05 the expected length of sub-harmonic edge waves L_k should be within 9–20 m, whereas L_k of synchronous edge waves should fall between 7–15 m. The above lengths of edge waves predict that cusp wavelengths equal $L_c = 0.5L_k \approx$ 5–10 m in the case of sub-harmonic and $L_c = L_k \approx$ 9–20 m for the synchronous edge waves. The comparison of dimensions of individual rhythmic forms, building the cusp system (L_c =6–18 m), observed in the field, with predictions using approximate values of standing edge wave parameters shows their substantial resemblance. Such a coincidence may to some extent point to the role of hydrodynamic, edge wave type forces in the formation of rhythmic shoreline undulations in the conditions of multi-bar, highly dissipative shore of a non-tidal Baltic Sea.

The above indicates that the nearshore area located in close shoreline proximity may exhibit reflective properties in small, local scales, despite the fact that the whole beach system is clearly dissipative on a larger scale. Naturally, for generally dissipative conditions, such as the analysed case, sub-harmonic or synchronous edge waves can only rarely become stable infragravity waves, so the resulting rhythmic shoreline forms are usually volatile and delicate.

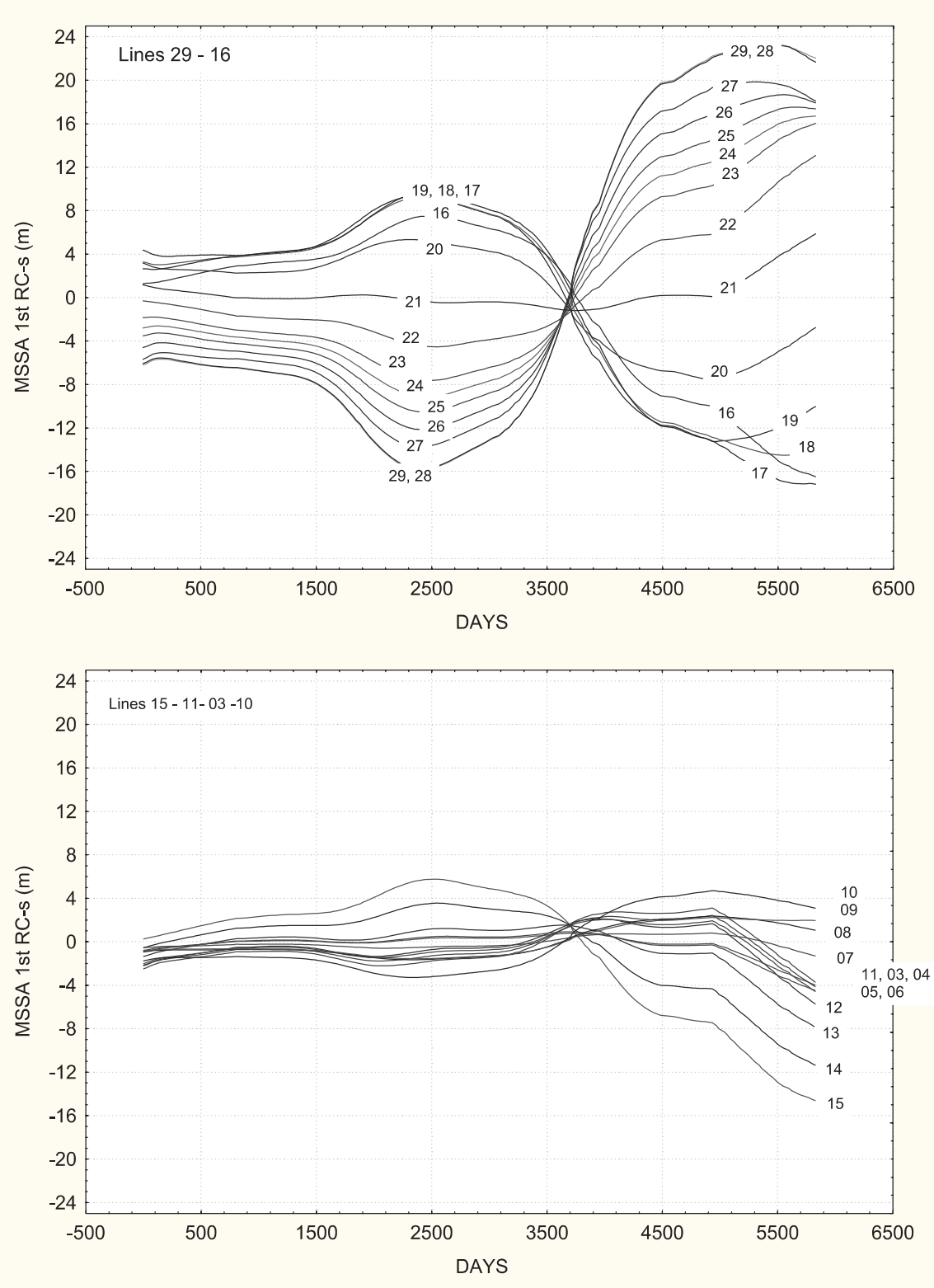

Fig. 14. First MSSA reconstructed component featuring standing wave with period of several decades

Positive correlations (relationships) between the generation and development of small cusps and the edge waves can only exist for relatively low wave intensity. When waves increase, cusps of the lengths of from several to ten metres or so disappear, but if the wave height decreases small cusps are once more generated. Such relations may prove that for larger waves there are negative couplings between the energy of edge waves and the emergence, development and stability of smaller cusps. When either swell or wind waves grow a bit and there is enough time for shoreline to adopt to a new hydrodynamic

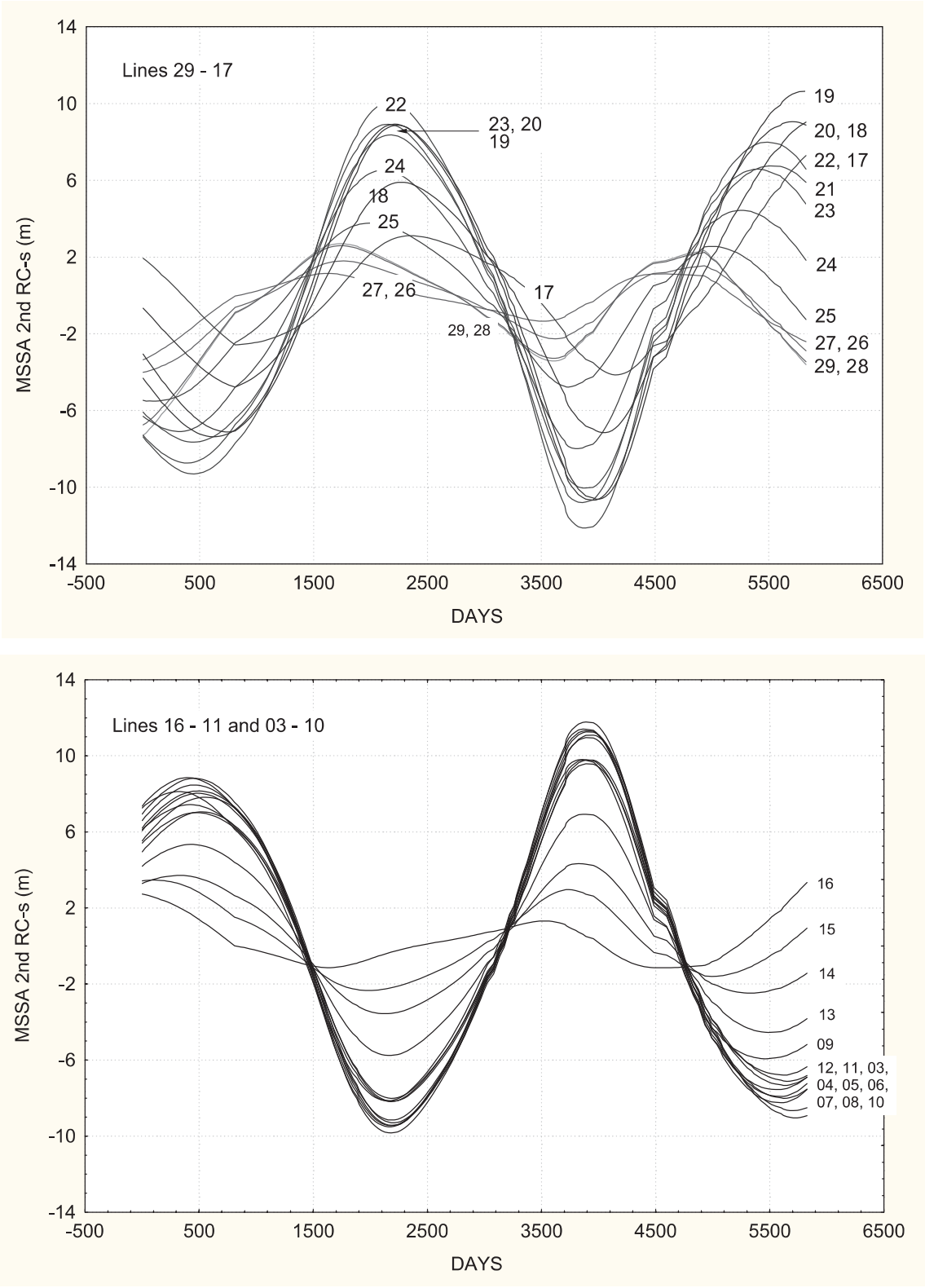

Fig. 15. Second MSSA reconstructed component featuring standing wave with period of 7–8 years

situation, small cusps, measuring several or tens of metres or so, turn into somewhat larger forms with several tens of meters. In such situations the observed spacing between cusp horns grows to 20–50 m and their amplitudes usually reach 1–2 m. However, persistence of both small and slightly larger cusps is generally still low and when they emerge, they can be rapidly transformed into other morphological entities or disappear. Further growth of wave intensity (beginning of storm) leads

to quick destruction of small and medium rhythmic shoreline forms. In such conditions the existence of larger scale quasi-rhythmic shoreline forms and seabed irregularities, as well as disturbances of wave and current fields (if any), can be manifested, apart from direct measurements, by visually observed alongshore variability of run-up patterns. Such observations reveal locations where waves can infiltrate into dry beach portions, which are bordered by drier adjacent areas.

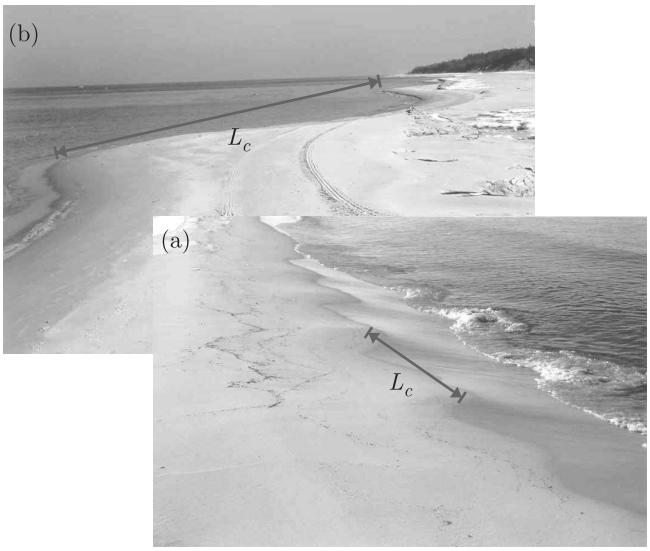

Fig. 16. Shoreline forms observed at CRS Lubiatowo

Soon after storms, particularly when swell prevails, apart from sections of regular smaller cusps, larger shoreline undulations with wavelengths of about 100–300 m are formed (Fig. 16b). This distance corresponds approximately to the then present surf zone width. These forms show both larger dimensions and greater persistence. The greatest stability though, is demonstrated by less regular embayments, whose shore dimensions are in the order of a kilometre and their cross-shore amplitudes measure several or tens of metres or so. The characteristic wavelengths of rhythmic shoreline undulations for 10 records of shoreline configurations are presented in Table 1. They were obtained from spectral analyses of individual, detrended shoreline records and were grouped into 5 classes, related to the lengths of measured coastal segments and sampling intervals of measurements. The associated deepwater wave characteristics correspond to the last daily hydrodynamic regimes just before shoreline records were taken. Table 1 shows that the most stable undulations have a wavelength $L_c \approx 1600$ m, which corresponds to the infragravity wave with $T_k \approx 120$ s and $L_c \approx 250$–350 m, matching $T_k \approx 30$ s and $L_c \approx 50$–150 m.

Discrete Wavelet Transform (DWT) analyses were executed to separate shoreline undulations of different lengths in order to investigate their individual characteristics. For example, the shoreline configurations between storms with the sampling rate $Deltax$ = 8.5 m revealed certain rhythmic features. Two components, which may represent shorter cusps were received for the wavelength bands of 17 m < $X1$ < 34 m and 35 m < $X2$ < 70 m. For the first filter the spectral analysis indicates the peak wavelength of $L_c^p \approx 20$ m. Since this peak is blurred, a certain wavelength band was adopted to contain the most important components ranging between 19 m < L_c < 23 m . The spectral analysis for the second component (35 m < $X2$ < 70 m) identifies the peak with $L_c^p \approx 47$ m and band of 40 m < L_c < 57 m. The choice of not only a peak value of L_c, but also inclusion of a certain wavelength band in its description, originates from the fact that the shoreline must continuously adapt to random and dynamically changing hydrodynamic conditions. The bands were thus defined upon the assumption that they should cover spectral estimates equal to at least 60% of a particular peak maximum. We deem wavelength bands to be more representative for the analysis and assessment of cusp morphology than single numbers of peak wavelengths. The adopted sampling rate (Δx = 8.5 m) put a limit for identification of the shortest cusps with wavelengths of just a few metres. For filters extracting longer wavelengths 70 m < $X3$ < 135 m, 136 m < $X4$ < 270 m and 275 m < $X5$ < 545 m the corresponding peak values were $L_c^p \approx 71$ m, $L_c^p \approx 170$ m and $L_c^p \approx 354$ m respectively. The L_c^p and L_c values can be interpreted as the basic multi-scale components describing shoreline rhythmicity during calm periods for wavelengths ranging between 20 m < L_c <550 m.

Table 1
Wavelengths of rhythmic shoreline undulations and deepwater wave parameters registered at CRS Lubiatowo in 2001 and 2003

No.	Date [d/m/y]	Surveyed shoreline length [m]	Samp. int. [m]	Wavelengths of rhythmic forms in sections [m]					Deepwater wave parameters	
				> 1000	500–1000	200–500	50–200	< 50	H_s [m]	T_p [s]
1	30/08/01	2500	50		500		160		0.3–0.6	4.1–5.4
2	04/10/01	2500	16	1600					0.7–1.3	4.2–5.2
3	17/04/03	2500	10	1600–2000			80	23	Unrecorded	Unrecorded
4	16/07/03	700	8.5				170	19, 40	Unrecorded	Unrecorded
5	17/07/03	2400	10	1500–2000			120, 65, 54	40	Unrecorded	Unrecorded
6	03/09/03	2400	10	1600–1900		250	85, 120		0.5–1.0	3.7–5.3
7	03/10/03	2400	8.5	1600–1900					0.3–1.1	3.5–4.8
8	19/10/03	7500	67.5	2000		280			0.4–1.2	3.7–6.0
9	12/11/03	7800	41	1650		340	185		0.2–0.3	2.6–3.6
10	26/11/03	2500	9.5	1700–1900		240	70		Unrecorded	Unrecorded

4. Concluding remarks

The major conclusions on the obtained achievements are summarised below:

– Gravity wave models worked out in the Lagrangian approach can be easily applied to simulation of different shallow-water wave phenomena including wave behaviour in the swash zone and orbital motion in the whole modelled area. Additionally, using the Lagrangian point of view some no-linear effects like non-sinusoidal wave shape and a wave driven current can be obtained already in the linear approach.
– Due to presence of the bar system, waves are subject to multiple breaking which causes wave energy dissipation and reduction of wave height. Thus, the bars protect the shore and the beach from the erosive impacts of storm waves. The spatial distribution of energy dissipation largely depends on deepwater wave height.
– In the south Baltic multi-bar coastal zone, two subsystems of bars can be distinguished. The first subsystem comprises inner bars, namely the first two stable bars, while the next bars constitute the outer system of bars, which behaves independently of the first one. The correlation between individual bars and between the shoreline and bars decreases in the offshore direction. The number of bars in the coastal zone depends on environmental passive factors, including mainly sediment diameter, while the shape and layout of bars is controlled by active parameters, associated with waves and currents, as well as wave transformation and breaking.
– At dissipative multi-bar shores of the south Baltic, edge waves occur in limited ranges of period. The field surveys carried out in Lubiatowo clearly revealed two slow varying components $T_k \approx 120$ s and $T_k \approx 30$ s during both relatively calm periods and storms. Higher frequencies (corresponding to T_k = 10–12 s) presumably represent sub-harmonic edge waves, because their periods match the double period of gravity wind waves that predominate at the Lubiatowo beach. The sub-harmonic edge waves, as well as synchronous edge waves (with the period equal to the period of wind waves), are believed to generate small shoreline forms, like beach cusps.
– Long term shoreline migration was found to consist of three standing waves with periods ranging between 7–8 years up to several decades and wavelengths between 1000 m and 1600 m. Each of them is present in the whole study area although only one is a dominant feature at any given location. They represent forced shoreline response to the wave climate; due to coincidence of periods the wave with $T = 8$ years can originate from the influence of the North Atlantic Oscillation.

Acknowledgements. The paper comprises results of fundamental research carried out within the thematic programme no. 2 of IBW PAN, which is hereby gratefully acknowledged.

REFERENCES

[1] Z Pruszak, G. Różyński, M. Szmytkiewicz, and R. Ostrowski, "Infragravity waves and rhythmic shoreline forms at a non-tidal, barred coast", *Proc. 29th International Conference on Coastal Engineering*, World Scientific Co. Pte. Ltd., 2568–2580 (2005).
[2] J. Kapiński, "Two-dimensional modelling of wave motion in shallow-water areas", *Archives of Hydro-Engineering and Environmental Mechanics* 51, 3–24 (2004).
[3] G. Różyński, "Long-term shoreline response of a nontidal, barred coast", *Coastal Engineering* 52, 79–91 (2005).
[4] R.T. Guza, and D. Inman, "Edge waves and beach cusps", *Journal of Geophysical Research* 80 (21), 2997–3012 (1975).
[5] G. Coco, D. Huntley, and T.J. O'Hare, "Beach cusp formation: analysis of a self -organisation model", *Coastal Sediments '99: The 4th International Symposium on Coastal Engineering and Science of Coastal Sediment Processes* (Hauppauge, New York, ASCE), 2190–2205 (1999).